Biophysical Journal Volume 108 June 2015 2759–2766

Biophysical Review

Axial Optical Traps: A New Direction for Optical Tweezers

Samuel Yehoshua,[1,2] Russell Pollari,[1,2] and Joshua N. Milstein[1,2,3,*]

[1]Department of Physics, University of Toronto, Toronto, Ontario, Canada; [2]Department of Chemical and Physical Sciences, University of Toronto Mississauga, Mississauga, Ontario, Canada; and [3]Institute of Biomaterials and Biomedical Engineering, University of Toronto, Toronto, Ontario, Canada

ABSTRACT Optical tweezers have revolutionized our understanding of the microscopic world. Axial optical tweezers, which apply force to a surface-tethered molecule by directly moving either the trap or the stage along the laser beam axis, offer several potential benefits when studying a range of novel biophysical phenomena. This geometry, although it is conceptually straightforward, suffers from aberrations that result in variation of the trap stiffness when the distance between the microscope coverslip and the trap focus is being changed. Many standard techniques, such as back-focal-plane interferometry, are difficult to employ in this geometry due to back-scattered light between the bead and the coverslip, whereas the noise inherent in a surface-tethered assay can severely limit the resolution of an experiment. Because of these complications, precision force spectroscopy measurements have adapted alternative geometries such as the highly successful dumbbell traps. In recent years, however, most of the difficulties inherent in constructing a precision axial optical tweezers have been solved. This review article aims to inform the reader about recent progress in axial optical trapping, as well as the potential for these devices to perform innovative biophysical measurements.

Optical tweezers provide a handle by which to interact with and manipulate the microscopic world, and since its inception some 30 years ago (1,2), the technique has continued to develop and evolve (3–5). Advances in optical force spectroscopy have yielded insight into a range of biological phenomena, such as the transport of cargo by molecular motors (6,7), the transcriptional procession of RNA polymerase (8,9), translational activity by ribosomes (10), and the packaging of DNA in bacteriophages (11). Optical tweezers typically function by generating an intense gradient force, arising from a tightly focused laser beam, to trap a dielectric particle attached to a molecule of interest. These instruments can be calibrated to an incredible level of precision, enabling the application of pico- to femtonewton forces while measuring subnanometer spatial displacements with microsecond temporal resolution (12).

One of the most successful implementations of optical tweezers is that of the dumbbell trap (6,13). In this case, a molecule is tethered between a pair of optically trapped microspheres (see Fig. 1 *A*). The configuration decouples the molecule from vibrational noise arising from the microscope stage (14), as well as from pointing instability of the laser, because both traps arise from the same light source (15). Dumbbell traps, however, have their own limitations, as the setup is often quite complicated and experimental throughput is limited to a single molecule. The limitations of a dumbbell trap become especially apparent when working with small molecules. Since the two traps can only be brought so close to one another before each microsphere begins to interact with the opposite trapping beam, one must either work with longer molecules or introduce some sort of linker molecule, such as a segment of DNA. The series elastic compliance of the linker molecules must be determined and factored into any analysis (15,16). However, because the linkers introduce thermal fluctuations that scale with the length of the tether (17), they will inevitably reduce the signal/noise ratio of the measurement (18).

A much simpler approach than the dumbbell trap is to tether one end of a molecule to a microscope coverslip, then optically trap a microsphere attached at the other end of the tether (see Fig. 1, *B* and *C*). Since only one optical trap is involved, the distance between the two tether points can be brought arbitrarily close together, overcoming one limitation of the dumbbell geometry. Another benefit of a single trap is that it should halve the amount of oxidative damage from singlet oxygen, which is known to be generated by the near-infrared trap light and the polystyrene microspheres, which can act as sensitizers (19). Furthermore, an advantage of surface-tethered assays is that because many molecules are simultaneously tethered, multiple molecules can be probed once the chamber is loaded. Some experiments on molecular motors or processive enzymes, for instance, where activity is initiated by the addition of NTPs to the chamber, would not benefit from this parallelism. However, in other experiments, such as studies of protein folding or protein-mediated DNA looping, these assays could prove effective. Unfortunately, due to a variety of complications with the conventional assays, the use of this geometry in precision optical force spectroscopy has been limited.

Submitted December 31, 2014, and accepted for publication May 13, 2015.

*Correspondence: josh.milstein@utoronto.ca

Editor: Brian Salzberg.

0006-3495/15/06/2759/8 $2.00

http://dx.doi.org/10.1016/j.bpj.2015.05.014

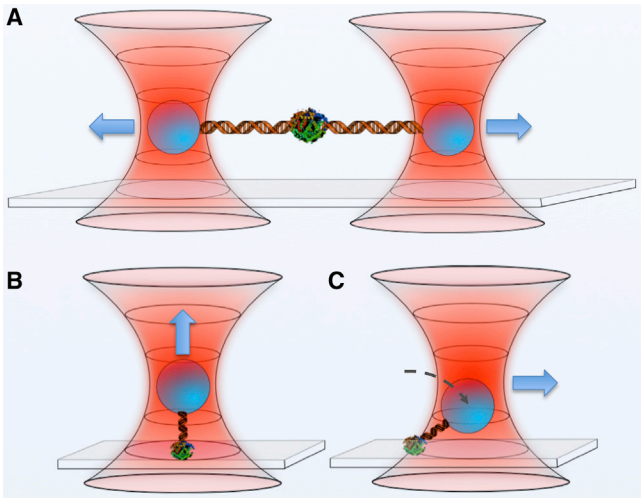

FIGURE 1 (*A*) Dumbbell optical traps are able to directly apply force to biological molecules along a single axis within the plane. (*B* and *C*) The direction of laser propagation is the natural axis along which to extend a surface-tethered molecule (*B*), but due to complications with this approach force is typically applied in a plane parallel to the coverslip (*C*). Unfortunately, the motion of the trapped microsphere and the optical force now couple to both the lateral and axial directions. To see this figure in color, go online.

In surface-tethered assays, the tendency is to apply force by moving the microsphere perpendicular to the direction of beam propagation (laterally) as opposed to along the axis of the laser (axially). For long tethers, the position of the microsphere within the harmonic potential of the trap, which yields the applied force, is straightforward to determine. However, for short tethers (<1 μm), great care has to be taken to obtain accurate force measurements (16). This is because the displacement of the microsphere within the optical trap, as the tether length is reduced, becomes increasingly coupled in both the lateral and axial directions (see Fig. 1 *C*). Since much of the force is now applied along the axial direction, the microsphere significantly shifts its distance above the coverslip, quickly entering a region where the trap is no longer well calibrated, and potentially crashing into the coverslip surface.

A solution to this problem is to simply extend the molecule along the direction of propagation, or axis, of the laser. Unfortunately, this approach suffers from a host of difficulties. Aberrations from the glass-liquid interface of the sample chamber as well as backscattered light between the bead and coverslip lead to a trapping potential that is a function of the height of the laser focus above the coverslip (20). Likewise, obtaining a precise measure of the trap height relative to the coverslip surface, as the trap is translated along the laser axis, poses its own challenges, as do high-speed measurements of bead displacement within the trap (such as back-focal-plane interferometry (21,22), which give optical tweezers their impressive temporal resolution). Moreover, by tethering one of the molecules to the microscope coverslip, the experiment is strongly coupled to the surrounding environment, which can introduce a significant amount of ambient noise into the collected data.

We note that this same axial geometry is used with magnetic tweezers, which have seen some remarkable technological advances in recent years (23). Magnetic tweezers can now apply forces similar to that of optical tweezers, are relatively simple to construct, have a throughput advantage, as multiple assays can be performed in parallel, and can be applied to very short molecules. However, when it comes to spatial and temporal resolution, optical tweezers are still far superior to magnetic tweezers. Fortunately, many of the challenges to utilizing axial optical tweezers in precision single-molecule measurements have been resolved by recent innovations, revealing axial tweezers as a powerful nascent biophysical technique. In this review article, our aim is to discuss the difficulties encountered in employing axial tweezers, present the techniques that have been devised to overcome these difficulties, and showcase some of the exciting biophysical explorations that are being undertaken with these unique new tools.

Stability and precision of surface-tethered assays

Dumbbell optical traps have traditionally been chosen as the technique of choice for precision force spectroscopy in large part because they are able to decouple from experimental noise, which can degrade a measurement. Confounding sources of error arise from noise in the trap and/or detection lasers, environmental sources such as vibrations and air currents, and mechanical and thermal drift. In the ideal case, free of measurement errors, the spatial resolution of an optical tweezers is limited only by thermal fluctuations that drive the Brownian motion of the trapped microsphere. The average position of the microsphere can be precisely determined at the cost of temporal resolution. If instrumental noise is negligible over the measurement period, the theoretical limit of spatial precision is on the order of Ångstroms (24). Despite the additional noise introduced by the fluctuations of a second trapped bead, this limit is achieved by dumbbell traps in a variety of ways, such as by monitoring cross correlations between the beads (17), applying active feedback control or, in the simplest approach, holding one of the beads in a very stiff trap that mimicks a surface (7).

Carter et al. recently showed that surface-coupled optical traps can also attain a spatial precision nearing the theoretical limit set by Brownian fluctuations (25). This atomic-scale sensitivity was achieved in two stages. The group first stabilized the sample to 0.1 nm in all three dimensions by continuously measuring the position of a local fiducial marker via back-focal-plane interferometry. These measurements were employed within a feedback loop to actively stabilize the sample set upon a three-axis piezostage. Second,

both the trap and detection lasers were sent through a single-mode polarization-maintaining optical fiber converting pointing, polarization, or mode noise in the laser into intensity noise. The output intensity was sampled and actively modulated by an acousto-optic modulator (AOM) placed before the input to the fiber, which greatly reduced the inherent noise of the lasers. With these modifications, Carter et al. were able to show basepair spatial sensitivity (0.34 nm) and enhanced force detection resolving force-induced changes of 0.1 pN in the unfolding dynamics of a DNA hairpin, all within a surface-coupled assay. Although dumbbell tweezers have been able to achieve sub-Ångstrom spatial resolution through elaborate means (such as passing the laser through low-refractive-index gas-filled chambers and maintaining 0.1 K temperature stability of the experimental apparatus (26)), surface-tethered assays can achieve performance comparable to that of most conventional dumbbell assays and in theory could attain such ultrastable performance if similar enhanced measures were taken.

Calibrating axial optical tweezers

To generate intense optical gradients, the majority of optical tweezers make use of oil-immersion high-NA objectives (NA >1.2). However, for biological specimens, optical trapping regularly occurs within an aqueous environment leading to a refractive index mismatch between the liquid solution ($n \sim 1.33$) and the immersion oil, which is typically chosen to match the coverglass ($n \sim 1.52$ for borosilicate glass). This mismatch results in both a focal shift and spherical aberrations that tend to elongate the focus of the laser along the axial direction (20). The focal shift can be estimated by the relation (27)

$$\frac{h_{\mathrm{NF}}}{h_{\mathrm{AF}}} \approx \sqrt{\left|\frac{(n_1)^2 - (\mathrm{NA})^2}{(n_2)^2 - (\mathrm{NA})^2}\right|}, \tag{1}$$

where h_{NF} is the nominal height of the focus about the coverslip, h_{AF} is the actual focal position, NA is the numerical aperture of the objective, and n_1, n_2 are the indices of refraction of the oil and the aqueous environment, respectively (see Fig. 2). The gradient force must compete with radiation pressure to form a stable trap. As one moves deeper within the sample chamber, elongation of the focal spot by spherical aberrations results in a reduced axial trap strength, so the actual trap center is positioned increasingly downstream of the focal spot. These effects can be alleviated by using water-immersion objectives (20), although the NA, and therefore the possible trap strength, of these objectives is limited compared to oil-immersion objectives.

A proper calibration of an axial tweezers system requires precise knowledge of where the trap center is in relation to the coverslip surface, as well as what the axial displacement is from the center of a trapped bead, and the resulting optical force on that bead. These are not trivial calibrations, since, in comparison to conventional optical tweezers, the trap stiffness is a function of axial position, as is the scattering intensity for a bead within the trap. A number of solutions have been found to account for these complications.

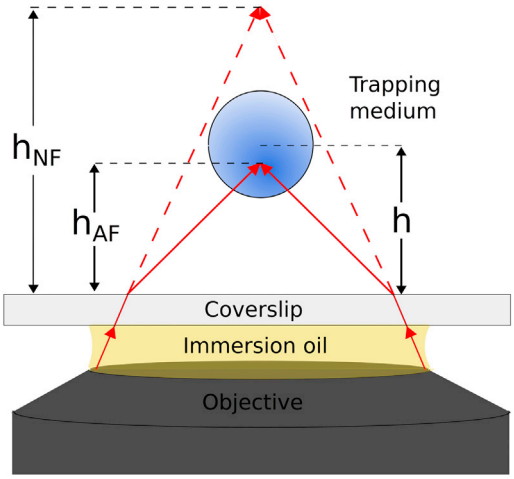

FIGURE 2 Oil-immersion objectives suffer from a mismatch in the indices of refraction between the immersion oil and the aqueous sample medium. In practice, the actual focal point, h_{AF}, is shifted below the nominal focal point, h_{NF}, of an index-matched system. Knowing the precise height, h, of an optically trapped microsphere above the coverslip is critical to surface-tethered assays. To see this figure in color, go online.

For instance, an estimate of the trap height, h, measured from the bead center to the surface can be attained by using Faxen's law, which provides a relationship for viscous drag, $\gamma_\perp$, as a function of proximity to a surface (28):

$$\gamma_\perp = \frac{\gamma_0}{1 - \frac{9R}{8h} + \frac{R^3}{2h^3} - \frac{57R^4}{100h^4} + \frac{R^5}{5h^5} + \frac{7R^{11}}{200h^{11}} - \frac{R^{12}}{25h^{12}}}, \tag{2}$$

where R is the bead radius and $\gamma_0 = 6\pi\eta R$ is the friction coefficient of a sphere in a fluid of viscosity η. Measurements of the power spectrum for an optically trapped bead, $S(f) = k_{\mathrm{B}}T/\pi^2\gamma_\perp(f^2 + f_{\mathrm{c}}^2)$, where $k_{\mathrm{B}}T = 4.1$ pN nm, can be taken at varying distances from the coverslip, and the data can be fit to yield a series of corner frequencies, f_{C}. The corner frequency quantifies the characteristic roll-off of the power spectrum and is given by the ratio of the trap stiffness, κ, to the viscous drag as $f_C = \kappa/2\pi\gamma_\perp$ (29). From this relationship, the data can then be fit to Faxen's law to provide a measure of the trap height. This method is not valid beyond ~2 μm from the surface, because at that distance, surface effects are miniscule. However, the real problem with this approach is that it assumes a constant trap strength, which is clearly problematic, so the method has limited applicability.

Deufel and Wang took the novel approach of using a well characterized molecular construct to calibrate an axial tweezers system (30). To measure the trap height above the

coverslip, which progressively shifts downward with stage displacement, Deufel and Wang first unzipped a 3.7 kbp sequence of double-stranded DNA (dsDNA) by extending the molecule along the axial direction. As each basepair sequentially denatured, the overall intensity signal, inferred through back-focal-plane interferometry, displayed a series of characteristic fluctuations with increasing trap height. The measured intensity fluctuations could be directly mapped onto the well-established, theoretical force-extension curve for the unzipping of dsDNA, providing an accurate relation between measured intensity and trap height from the coverslip surface throughout a 4 μm range. After calibrating the trap height, the dsDNA construct was again forced to unzip, but at much lower laser power, allowing the bead to move further from the trap center at each height. The measurements were then cross correlated to the well-established theoretical force-extension prediction to extract the relationship between measured intensity and displacement of the bead from the trap center. For bead displacements <~600 nm, the intensity signal displayed a linear relation for a range of laser powers.

Chen et al. (31) used a quite different approach that did not require an external construct for the calibrations. They first adapted a technique employed in magnetic tweezers experiments (32) to dynamically determine the bead-coverslip separation. Initially, a stuck bead was scanned through the optical trap, and a series of bright-field images of the bead were recorded on a CCD camera. The bead was imaged slightly out of focus so that it appeared as a dark spot with a bright ring of intensity around its edges. This donut-shaped intensity pattern could be fit by a polynomial, and a precise measure of the distance between the ring and the center of the microsphere was extracted at each axial position. A trapped microsphere was then imaged and compared to a fiducial bead stuck to the coverslip surface, providing a precise determination of the bead-coverslip separation ($\pm$1.4 nm). A related method was proposed by Dreyer et al. (33) to image the interference pattern of the forward-scattered laser light, within the back focal plane of the condenser, onto a CCD camera. Dreyer et al. were also able to determine the axial position of the bead to within a few nanometers (~3 nm). Of course, a limitation to both these techniques is that they employ a CCD camera, which limits the temporal resolution of the measurements to ~1 kHz. Ultra-high-speed cameras, in the range 1–100 kHz, are becoming increasingly available and affordable, but although they acquire images at rates approaching that of current detection schemes employing photodiodes, the vast amount of data they acquire and the consequent overhead involved in handling that data make video detection less preferable.

Chen et al. avoided the inherent complications of an extension-dependent trap strength by keeping the trap height fixed while at the same time trapping the bead within the linear region of the optical potential. In this way, varying the laser power would adjust the slope of the linear potential, resulting in an applied force. However, the real utility of trapping within the linear region of the potential is that it provides an all-optical force clamp in the axial direction. This trick was first employed by the Block lab (34), but in a dumbbell trapping geometry, to attain the sensitivity necessary to observe basepair stepping of RNA polymerase (26). To find and determine the extent of the linear part of the potential, Chen et al. built a dual-beam optical tweezers system with two beams of orthogonal polarization. The trap to be calibrated was held stationary while a much tighter probe trap moved a confined microsphere throughout the axial range of the stationary trap. By analyzing perturbations to the motion of the microsphere within the probe beam, the group could precisely map the optical potential.

Recently, Mack et al. proposed a method for performing axial optical tweezing that maintains the high temporal resolution afforded by position detection with a photodiode, but without the need to introduce an additional calibration construct (35). Their method makes use of the backscattering of light between the trapped bead and the coverslip surface, which gives rise to an oscillatory signal as the trap is translated axially (see Fig. 3). Mack et al. found that the background intensity pattern as a function of stage displacement, Δs, for an untethered yet optically trapped bead, is well described by the empirical fit:

$$I_{\mathrm{BG}} = P_{\mathrm{BG}}(\Delta s) + A_{\mathrm{BG}}\exp(-\lambda_{\mathrm{BG}}\, h(\Delta s))\sin(k\, h(\Delta s) + \phi_{\mathrm{BG}}). \quad (3)$$

Here, A_{BG}, ϕ_{BG}, λ_{BG}, and P_{BG} are fit parameters. $P_{\mathrm{BG}}(\Delta s)$ can be expressed in terms of a third-order polynomial in stage displacement, and $h(\Delta s)$, which is the bead coverslip separation for a free bead, can be written in terms of a

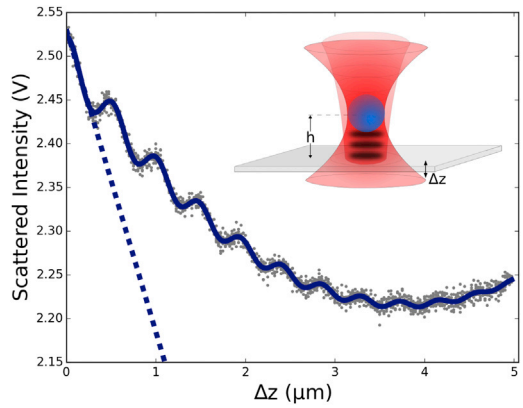

FIGURE 3 Scattering intensity versus axial stage displacement, Δz. The points (*solid line*) are the total measured (fitted) intensity signal for a trapped microsphere at different heights, h, above the coverslip, which displays a periodic modulation. The dashed line is for a microsphere stuck to the surface of the coverslip and is roughly linear. (*Inset*) Interference caused by back reflections between the microsphere and the coverslip surface. To see this figure in color, go online.

second-order polynomial in Δs. As previously observed in Neuman et al. (36), the oscillations in the intensity pattern display a periodicity with wavenumber $k = 4\pi/\lambda_W$, where λ_W is the wavelength of the trapping laser light in water. From this fit, they could accurately determine the trap height above the coverslip.

Mack et al. then repeatedly measured the power spectrum, fitting it to a Lorentzian distribution to attain the corner frequency, f_C, and diffusivity, $D_V \propto k_B T/\gamma_\perp$ (measured in $\langle V^2\rangle \mathrm{Hz}^{-1}$) of the bead at different bead-coverslip separations. The fits yielded both the trap stiffness, $\kappa = 2\pi f_C \gamma_\perp$, and the displacement sensitivity $\beta = D_V \gamma_\perp / k_B T$. The sensitivity β specifies the response of the measured intensity to changes in bead position with the bead-coverslip separation held constant, but during an axial force-extension measurement, this distance varies with molecular extension. For the intensity response of a bead displaced some distance, Δz, from the center of the trap, Mack et al. assumed a linear model of the form $I = I_{BG} - \zeta\, \Delta z$ and used the consistency relation $\beta = dI/dL$, where L is the molecule extension, to connect the response ζ to β. The resulting equations can be used to iteratively extract both the extension, L, and the displacement from the trap center, Δz, rapidly and with high accuracy.

Extending the range and increasing the trap strength

As an optical trap is moved deeper within a sample, the optical pressure arising from on-axis rays increasingly shifts the trap position further downstream from the focus, eventually overcoming the gradient force. This limits the maximum axial range of most optical traps to within ~20 μm from the surface (29). By comparing an oil- to a water-immersion objective, the latter of which correctly matches the refractive indices, Vermeulen et al. showed that the axial trap stiffness with a water-immersion objective displayed no height dependence (20). In fact, with water-immersion objectives, optical traps have been maintained to depths of ~150 μm.

Oil-immersion objectives, however, remain the preferred choice for many experiments. Their larger NA can generate tighter traps, although aberrations limit this improvement to trapping close to the coverslip surface (20). Of more critical importance, water-immersion objectives can be difficult to use, as the water layer between the objective and coverslip tends to evaporate over time, limiting extended-duration measurements. Moreover, the imaging gains of a higher-NA objective are necessary for some single-molecule experiments, for example, those involving objective total internal reflection fluorescence microscopy (37) in conjunction with optical force spectroscopy.

Much effort has been made to mitigate the aberration effects of oil-immersion objectives, both in optical trapping and in microscopy more generally. One approach, which is more of a compromise than a solution, is to more closely match the refractive index of the immersion oil to that of water, which can increase the axial trap stiffness by reducing aberrations and can also be used to fine-tune the trap height (38). Efforts to reduce spherical aberrations by directly engineering the focal spot, which include the use of spatial light modulators (39,40) and deformable membrane mirrors (41), offer a more promising solution, since wavefront modulations, although limited by the refresh rates of these devices, can be easily updated to reflect changes in trap height. For instance, Čižmár and colleagues were able to use shaped laser light to correct for all aberrations throughout the optical train (42). The ideal focus occurs when all modes of the laser arrive at the focal point with the same phase so as to constructively interfere. Čižmár et al. achieved this by using a phase-only spatial light modulator to directly optimize each mode in relation to an unmodified reference phase. With these corrections, they were able to create stable optical traps at milliwatt powers using low-NA, uncorrected objectives and to trap particles deep within a highly turbid medium, illustrating the power of this approach.

Reducing the optical pressure on a trapped particle can also lead to increased trap stiffness at much greater depths within a sample and can mitigate the effects of back-scattered light. The simplest approach is to reduce the intensity at the center of the beam by introducing a center field stop (43), but this method wastes much of the available laser power. A more efficient approach is to employ non-Gaussian modes of a laser to reduce the intensity at the beam center. Sato et al., for instance, employed the TEM_{01} mode, which is doughnut-shaped, to significantly increase the lateral trap stiffness. In addition, optical trapping with the TEM_{01} mode of the laser was later found to result in increased axial trap stiffness (up to approximately twofold) (44). Related strategies to increase the axial stiffness, such as trapping with radially polarized beams (45–47) or higher-order Laguerre-Gaussian modes (48,49), or a combination of the two (50), or with axicons (i.e., rotationally symmetrical prisms) (51), have also been implemented and have shown similar gains.

Alternatively, Zemánek et al. (52) demonstrated that strong axial traps can be created by a standing Gaussian wave. This was first realized by reflecting a laser beam off the mirrored top surface of a sample chamber to generate the standing wave (52,53). Small particles ($d < 0.1\ \lambda$) could be stably confined with the trap stiffness increased 10–100 times over that obtained using conventional optical tweezers (54). However, for larger particles ($d > 0.5\ \lambda$), which are associated with a concomitant increase in optical pressure, a standing wave trap quickly becomes unstable.

Prospects for axial optical traps

At present, axial optical tweezers have been applied toward only a limited number of biophysical measurements. Mack

et al. (35) employed the axial calibration they developed to study the winding and unwinding dynamics of the wild-type H4 nucleosome (55). Although experiments similar in scope have been performed on nucleosomes using conventional optical tweezers (56), their experiments nonetheless show the utility of an axial optical trap in performing precision single-molecule measurements.

Recently, Nawaz et al. made novel use of an axial optical tweezers to study the mechanical response of cells to piconewton forces (57). These experiments are conventionally performed with atomic force microscopy (AFM), but thermal noise experienced by the cantilever of the AFM when submerged in liquid limits the precision with which forces can be applied. Although the lower force limit for AFM is ~10 pN (3), AFM cell indentation experiments typically apply much larger forces (of order ~100 pN), because the lack of precision at low force makes it difficult to interpret the mechanical response. Conventional optical traps, which move in a plane parallel to the coverslip, could apply force to a cell by pressing upon it from the side with a trapped microsphere, which is quite different from AFM indentation experiments, where the pushing force is applied to the top of the cell. Axial traps, therefore, are a natural extension of the AFM experiments for probing the response to forces down to ~1 pN or less. Note, however, that Nawaz et al. were able to avoid many of the difficulties associated with axial tweezers, as discussed in this review, because the cells were large (and thus far enough from the surface that back-reflections were negligible) and only low forces were applied (so a water-immersion objective provided a suitable trap strength).

Precision axial optical tweezers could be used to explore the low-force regime of a variety of other measurements typically acquired via AFM, such as pull-out experiments, where individual polypeptides (or other membrane associated proteins) are pulled through various lipid bilayer domains (58). The stability of a membrane protein is governed both by forces that anchor the protein in the membrane and by forces that interact with the secondary structure of the protein. A classic example is the light-driven proton pump bacteriorhodopsin, one of the most extensively studied membrane proteins, which, along with adjacent lipids, forms a two-dimensional hexagonal lattice known as the purple membrane (59). Fine details of the inter- and intramolecular interactions might be accessible with axial tweezers that have not been resolvable with AFM (60). In a similar way, axial tweezers provide an ideal geometry for single-molecule measurements of binding or adhesion forces (on small molecules, proteins, or nanoparticles) without introducing a lateral or shearing force, which would be generated by conventional tweezers. Likewise, at the cellular level, axial tweezers could be used to map bacterial adhesion forces, as individual bacteria might be trapped and made to approach and retract from a perpendicular surface, simplifying the interpretation of these experiments (61).

Although the previous examples clearly show that axial optical tweezers lend themselves to applications where more conventional traps are inappropriate, another area in which axial tweezers have considerable potential is the direct measurement of single small biological molecules with enhanced force precision and a high signal/noise ratio. Chen et al. applied their optical force clamped axial tweezers to study the sensitivity of protein-mediated DNA loops of a few hundred basepairs to constant and fluctuating forces (62,63). Because of the extreme sensitivity of their instrument, they were able to resolve force-induced dynamical effects that resulted from applying only tens of femtonewtons of force. With this same instrument, they have been able to directly apply forces to DNA sequences as short as 250 basepairs (31), at which point sequence-dependent effects appeared (64).

Although optical tweezers are adept at finely resolving the motion and forces involved in, for instance, the translocation of a protein, single-molecule fluorescence techniques are more suited to uncovering the internal conformations of a protein of interest. Simultaneous fluorescence and optical force-spectroscopy measurements are complicated by the fact that the high-intensity lasers needed to create an optical trap quickly photobleach most fluorescent labels by two-photon processes. To get around this difficulty, the fluorescently labeled protein must be physically separated from the optical trap, which again requires the introduction of long linker molecules that degrade the precision of the measurement. Another approach is to temporally interleave both the trap and fluorescence excitation lasers so that the fluorophores are never in the excited state, where intersystem crossings occur, when the trap is on (65,66). Although this is an extremely powerful technique, the rapid switching (~66 kHz) and precision timing of the lasers and detection elements make this approach quite challenging to implement. A single-beam trap would be easier to temporally interlace with an excitation laser than would a dual-beam trap. Alternatively, axial tweezers might accommodate fluorescence measurements via a much simpler route. Since many of the techniques discussed here for increasing the strength and range of axial optical tweezers (employing the TEM_{01} mode, higher-order Laguerre-Gaussian modes, etc.) rely upon reducing the intensity in the central portion of the trap laser, a fluorescently labeled protein could be situated within this region that would remain at a much lower laser intensity throughout a force-extension measurement. For instance, Neupane et al. showed that a donut beam can be focused through a high-NA objective (NA 1.4) with a central intensity 20× less than the maximum value (67).

Since its inception, force spectroscopy with optical tweezers has proliferated in utility in the biophysical community. Although they are perhaps the most natural geometry for applying force with single-beam optical tweezers, axial tweezers have long been overlooked due to technical considerations that complicate their implementation. Now that

the fundamental challenges of using axial optical tweezers have been overcome, they will, hopefully, serve as a new and powerful addition to the single-molecule toolbox, helping us to gain an increasingly quantitative understanding of life's underlying mechanisms.

ACKNOWLEDGMENTS

We thank Christopher Yip as well as the anonymous reviewers for their detailed feedback on this article.

This research was funded by the Natural Sciences and Engineering Research Council of Canada (NSERC RGPIN 418251-13).

REFERENCES

1. Ashkin, A., J. M. Dziedzic, …, S. Chu. 1986. Observation of a single-beam gradient force optical trap for dielectric particles. *Opt. Lett.* 11:288–290.
2. Block, S. M., D. F. Blair, and H. C. Berg. 1989. Compliance of bacterial flagella measured with optical tweezers. *Nature.* 338:514–518.
3. Neuman, K. C., and A. Nagy. 2008. Single-molecule force spectroscopy: optical tweezers, magnetic tweezers and atomic force microscopy. *Nat. Methods.* 5:491–505.
4. Moffitt, J. R., Y. R. Chemla, …, C. Bustamante. 2008. Recent advances in optical tweezers. *Annu. Rev. Biochem.* 77:205–228.
5. Heller, I., T. P. Hoekstra, …, G. J. L. Wuite. 2014. Optical tweezers analysis of DNA-protein complexes. *Chem. Rev.* 114:3087–3119.
6. Finer, J. T., R. M. Simmons, and J. A. Spudich. 1994. Single myosin molecule mechanics: piconewton forces and nanometre steps. *Nature.* 368:113–119.
7. Svoboda, K., C. F. Schmidt, …, S. M. Block. 1993. Direct observation of kinesin stepping by optical trapping interferometry. *Nature.* 365:721–727.
8. Bintu, L., M. Kopaczynska, …, C. Bustamante. 2011. The elongation rate of RNA polymerase determines the fate of transcribed nucleosomes. *Nat. Struct. Mol. Biol.* 18:1394–1399.
9. Frieda, K. L., and S. M. Block. 2012. Direct observation of cotranscriptional folding in an adenine riboswitch. *Science.* 338:397–400.
10. Wen, J.-D., L. Lancaster, …, I. Tinoco. 2008. Following translation by single ribosomes one codon at a time. *Nature.* 452:598–603.
11. Smith, D. E., S. J. Tans, …, C. Bustamante. 2001. The bacteriophage straight ϕ29 portal motor can package DNA against a large internal force. *Nature.* 413:748–752.
12. Capitanio, M., and F. S. Pavone. 2013. Interrogating biology with force: single molecule high-resolution measurements with optical tweezers. *Biophys. J.* 105:1293–1303.
13. Visscher, K., S. P. Gross, and S. M. Block. 1996. Construction of multiple-beam optical traps with nanometer-resolution position sensing. *IEEE J. Sel. Top. Quantum Electron.* 2:1066–1076.
14. Shaevitz, J. W., E. A. Abbondanzieri, …, S. M. Block. 2003. Backtracking by single RNA polymerase molecules observed at near-base-pair resolution. *Nature.* 426:684–687.
15. Moffitt, J. R., Y. R. Chemla, …, C. Bustamante. 2006. Differential detection of dual traps improves the spatial resolution of optical tweezers. *Proc. Natl. Acad. Sci. USA.* 103:9006–9011.
16. Wang, M. D., H. Yin, …, S. M. Block. 1997. Stretching DNA with optical tweezers. *Biophys. J.* 72:1335–1346.
17. Meiners, J.-C., and S. R. Quake. 2000. Femtonewton force spectroscopy of single extended DNA molecules. *Phys. Rev. Lett.* 84:5014–5017.
18. Revyakin, A., R. H. Ebright, and T. R. Strick. 2005. Single-molecule DNA nanomanipulation: improved resolution through use of shorter DNA fragments. *Nat. Methods.* 2:127–138.
19. Landry, M. P., P. M. McCall, …, Y. R. Chemla. 2009. Characterization of photoactivated singlet oxygen damage in single-molecule optical trap experiments. *Biophys. J.* 97:2128–2136.
20. Vermeulen, K. C., G. J. L. Wuite, …, C. F. Schmidt. 2006. Optical trap stiffness in the presence and absence of spherical aberrations. *Appl. Opt.* 45:1812–1819.
21. Ghislain, L. P., N. A. Switz, and W. W. Webb. 1994. Measurement of small forces using an optical trap. *Rev. Sci. Instrum.* 65:2762–2768.
22. Gittes, F., and C. F. Schmidt. 1998. Interference model for back-focal-plane displacement detection in optical tweezers. *Opt. Lett.* 23:7–9.
23. De Vlaminck, I., and C. Dekker. 2012. Recent advances in magnetic tweezers. *Annu. Rev. Biophys.* 41:453–472.
24. Svoboda, K., and S. M. Block. 1994. Biological applications of optical forces. *Annu. Rev. Biophys. Biomol. Struct.* 23:247–285.
25. Carter, A. R., Y. Seol, and T. T. Perkins. 2009. Precision surface-coupled optical-trapping assay with one-basepair resolution. *Biophys. J.* 96:2926–2934.
26. Abbondanzieri, E. A., W. J. Greenleaf, …, S. M. Block. 2005. Direct observation of base-pair stepping by RNA polymerase. *Nature.* 438:460–465.
27. Carlsson, K. 1991. The influence of specimen refractive index, detector signal integration, and non-uniform scan speed on the imaging properties in confocal microscopy. *J. Microsc.* 163:167–178.
28. Schäffer, E., S. F. Nørrelykke, and J. Howard. 2007. Surface forces and drag coefficients of microspheres near a plane surface measured with optical tweezers. *Langmuir.* 23:3654–3665.
29. Neuman, K. C., and S. M. Block. 2004. Optical trapping. *Rev. Sci. Instrum.* 75:2787–2809.
30. Deufel, C., and M. D. Wang. 2006. Detection of forces and displacements along the axial direction in an optical trap. *Biophys. J.* 90:657–667.
31. Chen, Y.-F., G. A. Blab, and J.-C. Meiners. 2009. Stretching submicron biomolecules with constant-force axial optical tweezers. *Biophys. J.* 96:4701–4708.
32. Revyakin, A., J. F. Allemand, …, T. R. Strick. 2003. Single-molecule DNA nanomanipulation: detection of promoter-unwinding events by RNA polymerase. *Methods Enzymol.* 370:577–598.
33. Dreyer, J. K., K. Berg-Sørensen, and L. Oddershede. 2004. Improved axial position detection in optical tweezers measurements. *Appl. Opt.* 43:1991–1995.
34. Greenleaf, W. J., M. T. Woodside, …, S. M. Block. 2005. Passive all-optical force clamp for high-resolution laser trapping. *Phys. Rev. Lett.* 95:208102.
35. Mack, A. H., D. J. Schlingman, …, S. G. J. Mochrie. 2012. Practical axial optical trapping. *Rev. Sci. Instrum.* 83:103106.
36. Neuman, K. C., E. A. Abbondanzieri, and S. M. Block. 2005. Measurement of the effective focal shift in an optical trap. *Opt. Lett.* 30:1318–1320.
37. Axelrod, D. 1989. Total internal reflection fluorescence microscopy. *Methods Cell Biol.* 245–270.
38. Reihani, S. N. S., and L. B. Oddershede. 2007. Improving optical trapping in the axial direction and a continuous change of the optimal trapping depth. *Proc. SPIE Int. Soc. Opt. Eng.* 6644:664421–664428.
39. Wulff, K. D., D. G. Cole, …, M. J. Padgett. 2006. Aberration correction in holographic optical tweezers. *Opt. Express.* 14:4170–4175.
40. Sinclair, G., P. Jordan, …, J. Cooper. 2004. Defining the trapping limits of holographical optical tweezers. *J. Mod. Opt.* 51:409–414.
41. Theofanidou, E., L. Wilson, …, J. Arlt. 2004. Spherical aberration correction for optical tweezers. *Opt. Commun.* 236:145–150.
42. Čižmár, T., M. Mazilu, and K. Dholakia. 2010. In situ wavefront correction and its application to micromanipulation. *Nat. Photonics.* 4:388–394.

43. Gussgard, R., T. Lindmo, and I. Brevik. 1992. Calculation of the trapping force in a strongly focused laser beam. *J. Opt. Soc. Am. B.* 9:1922–1930.

44. Friese, M. E., H. Rubinsztein-Dunlop, …, E. W. Dearden. 1996. Determination of the force constant of a single-beam gradient trap by measurement of backscattered light. *Appl. Opt.* 35:7112–7116.

45. Zhan, Q. 2003. Radiation forces on a dielectric sphere produced by highly focused cylindrical vector beams. *J. Opt. A, Pure Appl. Opt.* 5:229–232.

46. Zhan, Q. 2004. Trapping metallic Rayleigh particles with radial polarization. *Opt. Express.* 12:3377–3382.

47. Nieminen, T. A., N. R. Heckenberg, and H. Rubinsztein-Dunlop. 2008. Forces in optical tweezers with radially and azimuthally polarized trapping beams. *Opt. Lett.* 33:122–124.

48. Simpson, N. B., L. Allen, and M. J. Padgett. 1996. Optical tweezers and optical spanners with Laguerre-Gaussian modes. *J. Mod. Opt.* 43:2485–2491.

49. Simpson, N. B., D. McGloin, …, M. J. Padgett. 1998. Optical tweezers with increased axial trapping efficiency. *J. Mod. Opt.* 45:1943–1949.

50. Kawauchi, H., K. Yonezawa, …, S. Sato. 2007. Calculation of optical trapping forces on a dielectric sphere in the ray optics regime produced by a radially polarized laser beam. *Opt. Lett.* 32:1839–1841.

51. Lei, M., Z. Li, …, T. Ye. 2013. Long-distance axial trapping with focused annular laser beams. *PLoS ONE.* 8:e57984.

52. Zemánek, P., A. Jonáš, …, M. Liška. 1998. Optical trapping of Rayleigh particles using a Gaussian standing wave. *Opt. Commun.* 151:273–285.

53. Zemánek, P., A. Jonáš, …, M. Liška. 2003. Theoretical comparison of optical traps created by standing wave and single beam. *Opt. Commun.* 220:401–412.

54. Trojek, J., V. Karásek, and P. Zemánek. 2009. Extreme axial optical force in a standing wave achieved by optimized object shape. *Opt. Express.* 17:10472–10488.

55. Mochrie, S. G., A. H. Mack, …, L. Regan. 2013. Unwinding and rewinding the nucleosome inner turn: force dependence of the kinetic rate constants. *Phys. Rev. E Stat. Nonlin. Soft Matter Phys.* 87:012710.

56. Mihardja, S., A. J. Spakowitz, …, C. Bustamante. 2006. Effect of force on mononucleosomal dynamics. *Proc. Natl. Acad. Sci. USA.* 103:15871–15876.

57. Nawaz, S., P. Sánchez, …, I. A. T. Schaap. 2012. Cell visco-elasticity measured with AFM and optical trapping at sub-micrometer deformations. *PLoS ONE.* 7:e45297.

58. Kessler, M., and H. E. Gaub. 2006. Unfolding barriers in bacteriorhodopsin probed from the cytoplasmic and the extracellular side by AFM. *Structure.* 14:521–527.

59. Haupts, U., J. Tittor, and D. Oesterhelt. 1999. Closing in on bacteriorhodopsin: progress in understanding the molecule. *Annu. Rev. Biophys. Biomol. Struct.* 28:367–399.

60. Oesterhelt, F., D. Oesterhelt, …, D. J. Müller. 2000. Unfolding pathways of individual bacteriorhodopsins. *Science.* 288:143–146.

61. Evans, E. A., and D. A. Calderwood. 2007. Forces and bond dynamics in cell adhesion. *Science.* 316:1148–1153.

62. Chen, Y.-F., J. N. Milstein, and J.-C. Meiners. 2010. Femtonewton entropic forces can control the formation of protein-mediated DNA loops. *Phys. Rev. Lett.* 104:048301.

63. Chen, Y.-F., J. N. Milstein, and J.-C. Meiners. 2010. Protein-mediated DNA loop formation and breakdown in a fluctuating environment. *Phys. Rev. Lett.* 104:258103.

64. Raghunathan, K., Y.-F. Chen, …, J.-C. Meiners. 2011. Mechanics of DNA: sequence dependent elasticity. *Proc. SPIE Int. Soc. Opt. Eng.* 8097:80970C.

65. Brau, R. R., P. B. Tarsa, …, M. J. Lang. 2006. Interlaced optical force-fluorescence measurements for single molecule biophysics. *Biophys. J.* 91:1069–1077.

66. Comstock, M. J., T. Ha, and Y. R. Chemla. 2011. Ultrahigh-resolution optical trap with single-fluorophore sensitivity. *Nat. Methods.* 8: 335–340.

67. Neupane, B., F. Chen, …, G. Wang. 2013. Tuning donut profile for spatial resolution in stimulated emission depletion microscopy. *Rev. Sci. Instrum.* 84:043701.